Cells and Materials

Volume 3 | Number 4 Article 8

1993

Influence of Crystal Structure on the Establishment of the Bone-Calcium Phosphate Interface In Vitro

J. D. de Bruijn
University of Leiden, The Netherlands

C. P. A. T. Klein
University of Leiden, The Netherlands

K. de Groot
University of Leiden, The Netherlands

C. A. van Blitterswijk
University of Leiden, The Netherlands

Cells and Materials, Vol. 3, No. 4, 1993 (Pages 407-417)
Scanning Microscopy International, Chicago (AMF O'Hare), IL 60666 USA

1051-6794/93$5.00+.00

INFLUENCE OF CRYSTAL STRUCTURE ON THE ESTABLISHMENT OF THE BONE-CALCIUM PHOSPHATE INTERFACE *IN VITRO*

J.D. de Bruijn*, C.P.A.T. Klein, K. de Groot and C.A. van Blitterswijk

Laboratory for Otobiology & Biocompatibility, Biomaterials Research Group, University of Leiden, Rijnsburgerweg 10, 2333 AA Leiden, The Netherlands

(Received for publication July 30, 1993, and in revised form December 8, 1993)

Abstract

An *in vitro* rat bone marrow cell system was used to examine the interfacial ultrastructure established between various calcium phosphates and mineralized tissue. The investigated calcium phosphates comprised hydroxyapatite (HA), fluorapatite (FA), tricalcium phosphate (TCP), tetracalcium phosphate (TECP) and magnesium whitlockite (MWL). Both scanning and transmission electron microscopy were used to examine the elaborated interface. The time in which a mineralized extracellular matrix was formed on the various materials differed from 2 weeks on HA, TCP and TECP, to 8 weeks on FA. It was only occasionally observed in some areas on MWL, which might have been due to aluminum impurities in the coating. With transmission electron microscopy, three distinct interfacial structures were observed. They differed in the presence or absence of a collagen free, 0.7 to 0.8 μm wide, amorphous zone and a 20 to 60 nm thick electron dense layer, interposed between the material surface and the mineralized extracellular matrix. The electron dense layer was considered to be at least partially caused by protein adsorption, which would precede or concur with biological mineralization events, while the amorphous zone was regarded to represent partial degradation of the calcium phosphate surfaces. The results of this study show that plasma sprayed calcium phosphates will display different bone-bonding and biodegradation properties, depending on their chemical composition and crystal structures.

Key Words: Calcium phosphate, hydroxyapatite, interface, bone formation, *in vitro*, mineralization, osteoblast, plasma spray.

*Address for correspondence:
Joost D. de Bruijn,
Laboratory for Otobiology & Biocompatibility,
Building 55, Biomaterials Research Group,
University of Leiden, Rijnsburgerweg 10,
2333 AA Leiden,
The Netherlands

Telephone number: 31-71-276420
FAX number: 31-71-276437

Introduction

Calcium phosphate ceramics are widely used as bone replacement materials in orthopaedic surgery, dentistry, otolaryngology, and reconstructive surgery due to their bone bonding capacities [Jarcho, 1981; Ganeles *et al.*, 1985; van Blitterswijk *et al.*, 1985; LeGeros, 1988]. Since these ceramics have to fulfill certain requirements for each implantation site, such as the degree of dissolution, a range of defined materials is needed. For calcium phosphates, different material properties can be achieved by varying the chemical composition, or crystallography [de Groot *et al.*, 1985], and crystallinity [de Bruijn *et al.*, 1993]. By changing the calcium/phosphorous ratio or by the addition of ions, such as magnesium and fluorine, the chemical composition will be altered with the resulting effects on biodegradation [Klein *et al.*, 1983]. It has been reported that by the substitution of fluorine for the hydroxyl ions in hydroxyapatite, fluorapatite forms, which has a lower solubility rate than hydroxyapatite [Moreno *et al.*, 1977; Heling *et al.*, 1981; LeGeros, 1981; Lugscheider *et al.*, 1988]. Another advantage of fluorapatite is its stability at high temperatures, and therefore, its suitability for plasma spraying [Lugscheider *et al.*, 1988]. Incorporation of magnesium in calcium phosphates, to form magnesium whitlockite, has also been reported to reduce the *in vitro* dissolution rate [Klein *et al.*, 1986; Driessens, 1988]. Recent experiments by Dhert *et al.* (1993) have shown a satisfactory biocompatibility of fluorapatite and magnesium whitlockite plasma-sprayed coatings in bone tissue, however, based on push-out tests, a better implant fixation was seen with the former.

Not only the addition of ions, but also the change in Ca/P ratio has been reported to affect the biodegradation rate of calcium phosphates. Several studies with tricalcium phosphate have shown its good biocompatibility, osteoconductivity and high dissolution rate [Klein *et al.*, 1983, 1986, 1991; de Groot *et al.*, 1985]. It was suggested by Klein *et al.* (1991), that the high dissolution rate of plasma sprayed tricalcium phosphate caused more bone remodelling and/or formation of connective tissue along the interface when implanted in dog femora for 3 months. Conversely, the high dissolution rate that

was observed with plasma-sprayed tetracalcium phosphate coatings, was suggested to induce reprecipitation of hydroxyapatite on its surface, resulting in considerable bone contact.

There is a general assumption that surface active materials, characterized by their ability to form a surface apatite layer, will give rise to the formation of mineralized tissue more rapidly on their surface as compared to inert materials. There are additional suggestions that highly crystalline hydroxyapatite and fluorapatite might be regarded as having very low surface active properties. If this is correct, differences in mineralized tissue formation would be expected on calcium phosphates with varying degradation rates, and thus different chemical compositions and crystal structures. The aim of the present study was to examine the effect of chemical composition and crystallography of plasma-sprayed calcium phosphate coatings on the establishment and nature of the bone-coating interface.

Materials and Methods

Calcium phosphate coatings

Five calcium phosphates, differing in crystal structure and chemical composition were plasma-sprayed as a 20 to 50 μm thick layer onto 13 mm round coverslips (Thermanox®). The materials included hydroxyapatite and fluorapatite (both of which were supplied by CAM-Implants BV, Leiden, The Netherlands and Merck BV, The Netherlands), tricalcium phosphate and magnesium whitlockite (both supplied by ECN, Petten, The Netherlands), and tetracalcium phosphate (supplied by BK-Ladenburg, Germany). All materials were sterilized with ^{60}Co gamma irradiation (2.5 MRad) prior to cell culture.

Rat bone marrow cell isolation and culture

Rat bone marrow cells were obtained from 100-120 g young adult male Wistar rats according to the method described by Maniatopoulos *et al.* (1988). Cells removed from each femur were grown in α-minimal essential medium (α-MEM-RNA/DNA, Gibco), supplemented with antibiotics (100 U/ml penicillin and 100 μg/ml streptomycin, Boehringer-Mannheim), 15% foetal calf serum (FCS) and freshly prepared 50 μg/ml ascorbic acid, 10 mM ß-glycerophosphate (both Gibco) and 10^{-8} M dexamethasone (Sigma). After 5 days of primary culture, subcultured cells were seeded at a concentration of 1×10^4 cells/cm^2 on the different plasma-sprayed substrata {7 samples per material per time; 3 for scanning (SEM) and 4 for transmission electron microscopy (TEM)}. Cultures were refed every other day, and maintained for 1, 2, 4 and 8 weeks at 37°C, in a humidified atmosphere of 90% air and 10% CO_2. Control specimens were incubated in supplemented culture medium without the presence of cells. After the culture period, the cells were fixed and processed for SEM and TEM.

Table 1. Interfacial structures and mineralization.

	HA	FA	TECP	TCP	MWL
amorphous/ degrading zone	+	-	+	-	-
electron dense layer	+	±	+	±	-
mineralization (weeks)	2	8	2	2	-

Scanning electron microscopy (SEM)

Prior to fixation, cells were washed three times in α-MEM at 37°C, without serum added and then twice with 0.1 M Na-cacodylate buffer (pH 7.4, 37°C). Fixation was carried out for 45 minutes at room temperature in 1.5% glutaraldehyde in the same buffer. This was followed by dehydration in a graded series of ethanol and critical point drying from carbon dioxide (Balzers model CPD 030). Overlying cell layers were removed with compressed air or adhesive tape to facilitate examination of the elaborated mineralized extracellular matrix. All specimens were subsequently sputter coated with gold (Balzers MED 010) and examined in a Philips S 525 SEM (equipped with a X-ray microanalysis capability, Voyager XRMA system, Noran Instruments) operated at an accelerating voltage of 15 kV.

Transmission electron microscopy (TEM)

Cells were washed as described above, and fixed in Karnovsky's fixative, containing 1.5% paraformaldehyde and 2% glutaraldehyde in 0.1 M Na-cacodylate buffer, pH 7.4, for 2 hours at 4°C. After washing in the same buffer, cells were post-fixed in a freshly prepared aqueous solution of 1.5% potassium ferrocyanide and 1% osmium tetroxide, for 16 hours at 4°C, to enhance membrane contrast.

Cultures that were stained for glycosaminoglycans, were pre- and post-fixed in the presence of ruthenium red, according to the method described by Luft (1971). Samples were dehydrated through a graded series of ethanol and embedded in Epon. Ultra-thin sections were processed on a LKB ultramicrotome, routinely contrast stained with uranyl acetate and lead citrate, and examined in a Philips EM 201 or EM 400 TEM operated at an acceleration voltage of 80 kV.

Results

Cells adhered and spread on all the materials and after one week of culture, several areas could be distinguished in which a higher concentration of cells was present. In these nodules and in the surrounding cell multilayer, a collagenous extracellular matrix was observed with SEM. The cell multi-layers on magnesium whitlockite and tissue culture polystyrene were frequently

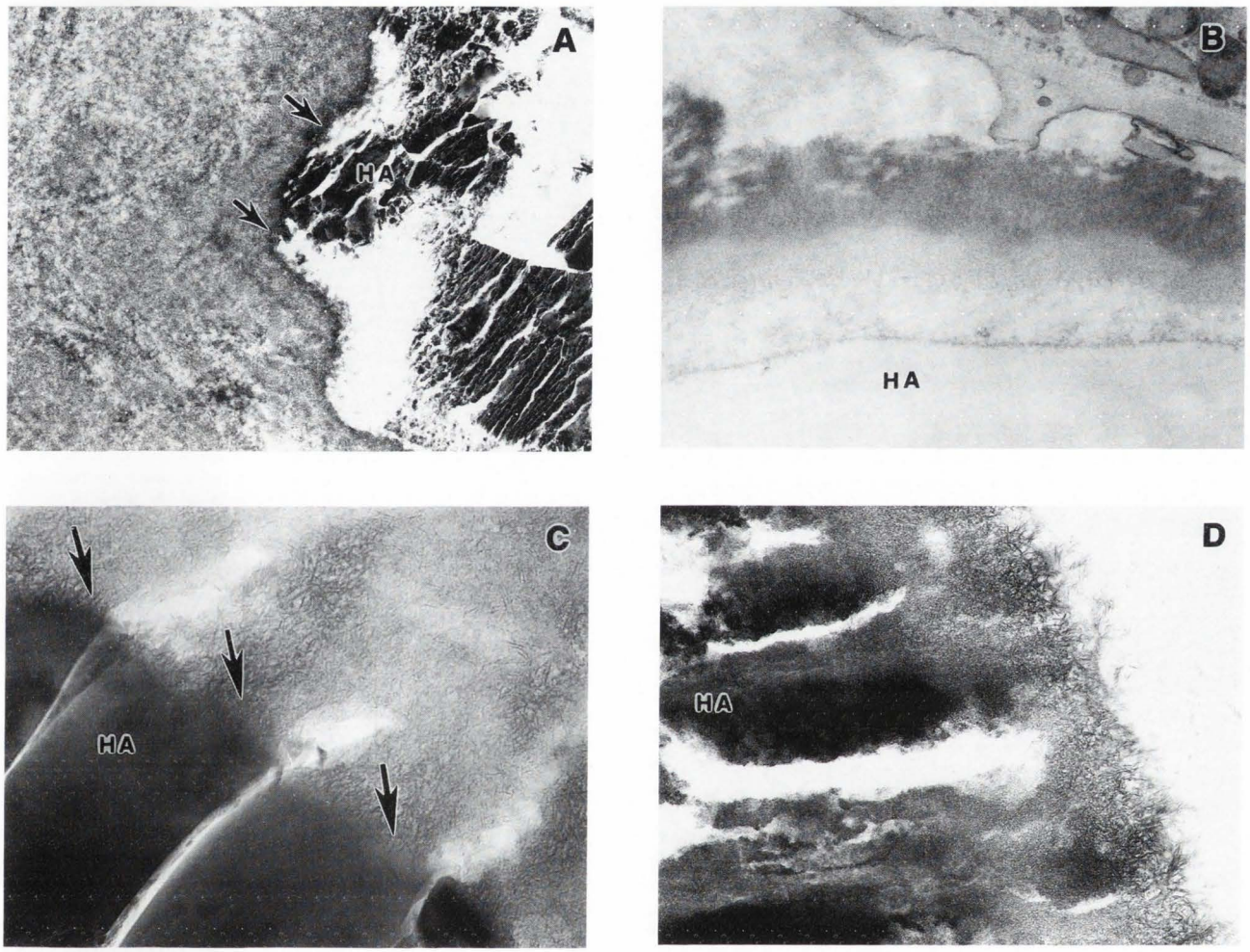

Figure 1. A. Undecalcified section showing an electron dense layer (arrows) at the interface between the mineralized extracellular matrix and the hydroxyapatite (HA) surface. **B**. Ruthenium red stained sample showing an unstained interfacial zone between the hydroxyapatite "ghost" surface (HA) and the positively stained extracellular matrix. **C**. There is an intimate contact between needle shaped crystals from the mineralized extracellular matrix and the hydroxyapatite surface (arrows). **D**. Degradation of the hydroxyapatite surface resulting in the absence of a clear transition between the material and the mineralized extracellular matrix. Field widths: (A) 6.6 μm; (B) 3.3 μm; (C) 0.9 μm; and (D) 2.2 μm.

---

lost during the critical point drying procedure, which indicated that they were loosely attached. Conversely, on tricalcium phosphate, tetracalcium phosphate, hydroxyapatite, and fluorapatite, the cell multi-layer was firmly attached and could only be partially removed with compressed air or adhesive tape. Table 1 summarizes the interfacial structures observed between mineralized matrix and the various calcium phosphates, and the time at which they were formed on the different materials. A more detailed description of the elaborated interfaces between mineralized extracellular matrix and the various calcium phosphates, as seen by SEM and TEM, is given below.

Hydroxyapatite

Scanning electron microscopy showed a slight change in surface texture of the hydroxyapatite coating after two weeks of culture, in that small cavities became apparent. A mineralized extracellular matrix had already been formed in several areas, which became more abundant after 4 weeks of culture. Transmission electron microscopy revealed that the mineralized extracellular matrix had been directly deposited onto the hydroxyapatite surface. At this interface, a 20-60 nm thick electron dense layer was frequently observed (Fig. 1A). Needle-shaped crystals were in direct contact with the hydroxyapatite surface (Fig. 1C), which sometimes showed severe signs of degradation (Fig. 1D). Here, the hydroxyapatite surface had changed into a more granular, amorphous character, in which no clear transition was seen between the biomaterial and the mineralized

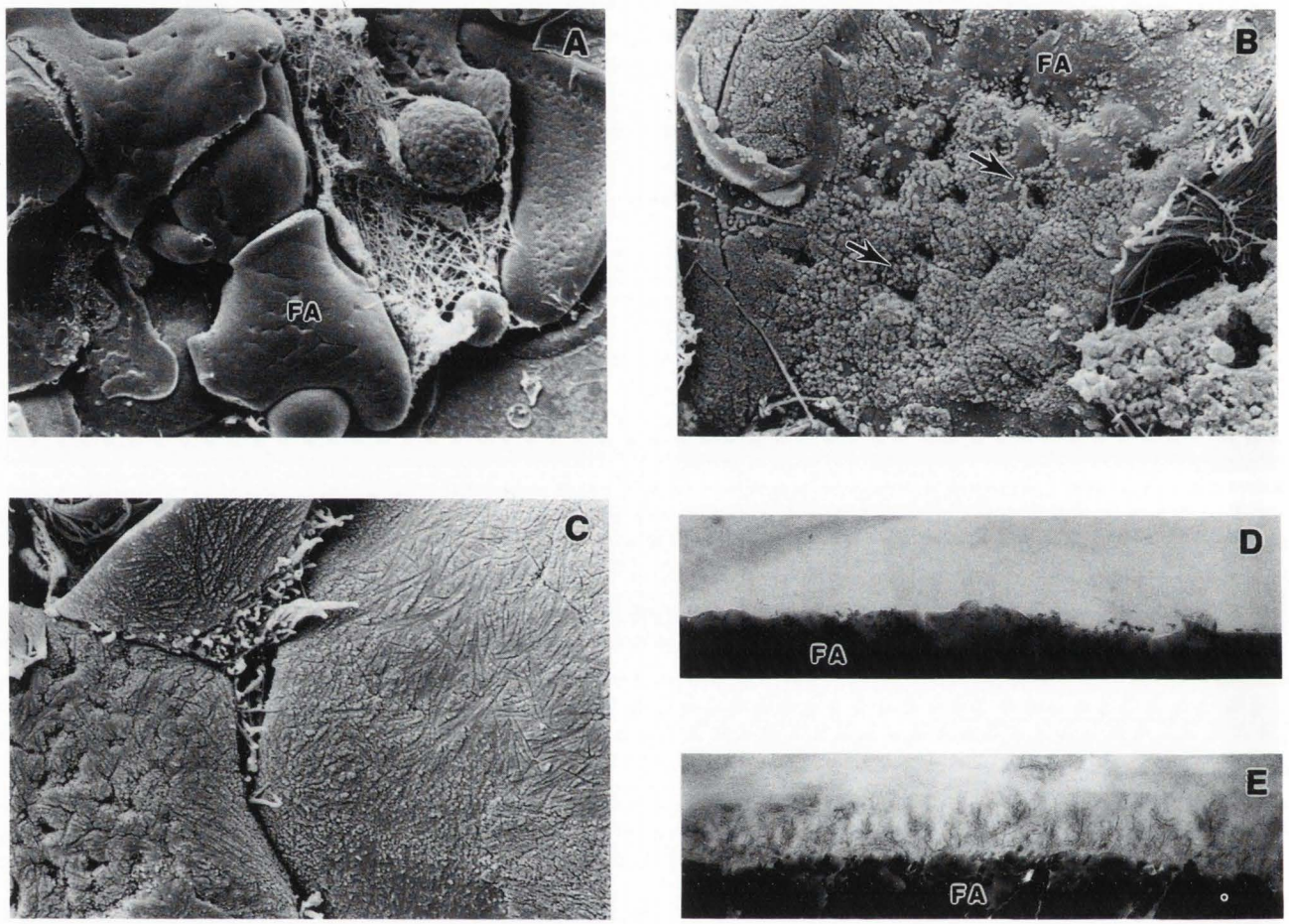

Figure 2. A. Scanning electron micrograph showing a largely unaltered fluorapatite (FA) surface after 2 weeks of culture. **B and C**. At 8 weeks, globular accretions (arrows) have accumulated at the surface of fluorapatite (FA), incorporating collagen fibres **(C)**. **D and E**. Transmission electron micrographs of the fluorapatite surface after 2 weeks **(D)** and 8 weeks **(E)** of culture, the latter showing mineralization on to the fluorapatite (FA) surface. Field widths: (A) 61 μm; (B) 16.3 μm; (C) 15.6 μm; (D) 1.5 μm; and (E) 2.2 μm.

extracellular matrix. Decalcified specimens that had been stained with ruthenium red, frequently revealed an amorphous zone interposed between the hydroxyapatite surface and the positively stained extracellular matrix (Fig. 1B).

Fluorapatite

After two weeks of culture, an unmineralized collagenous extracellular matrix was observed on the surface of the fluorapatite coatings (Fig. 2A). A similar appearance was seen at 4 weeks, and mineralization of the fluorapatite surface was only seen at 8 weeks of culture (Figs. 2B-2D). Small globular deposits, with a diameter of up to 0.1 μm were seen randomly distributed over the fluorapatite surface (Fig. 2B). In several areas, these globular deposits had merged to form a continuous layer, to which collagen fibres were attached (Fig. 2C). Transmission electron microscopy also revealed mineralization onto the fluorapatite surface, only after 8 weeks of culture (Figs. 2D and 2E), while the fluorapatite was still composed of large crystallites.

Tetracalcium phosphate

The surface of the tetracalcium phosphate coatings showed a clear change in surface morphology after 2 weeks of culture (Figs. 3A and 3B). Cracks and small cavities appeared and plate-like structures became visible. The surrounding extracellular matrix showed numerous mineralization foci interwoven with collagen fibres. The surface of the tetracalcium phosphate was fully covered with mineralized extracellular matrix after 4 weeks of culture and collagen fibres were attached to its surface (Figs. 3C and 3D). Transmission electron microscopy revealed a gel-like, amorphous zone interposed between the tetracalcium phosphate surface and the mineralized extracellular matrix which partially represented the degrading surface of the tetracalcium phosphate (Fig. 4A). This zone was devoid of collagen fibres and had an average thickness of approximately 800 nm. An electron dense layer was frequently distinguished between the

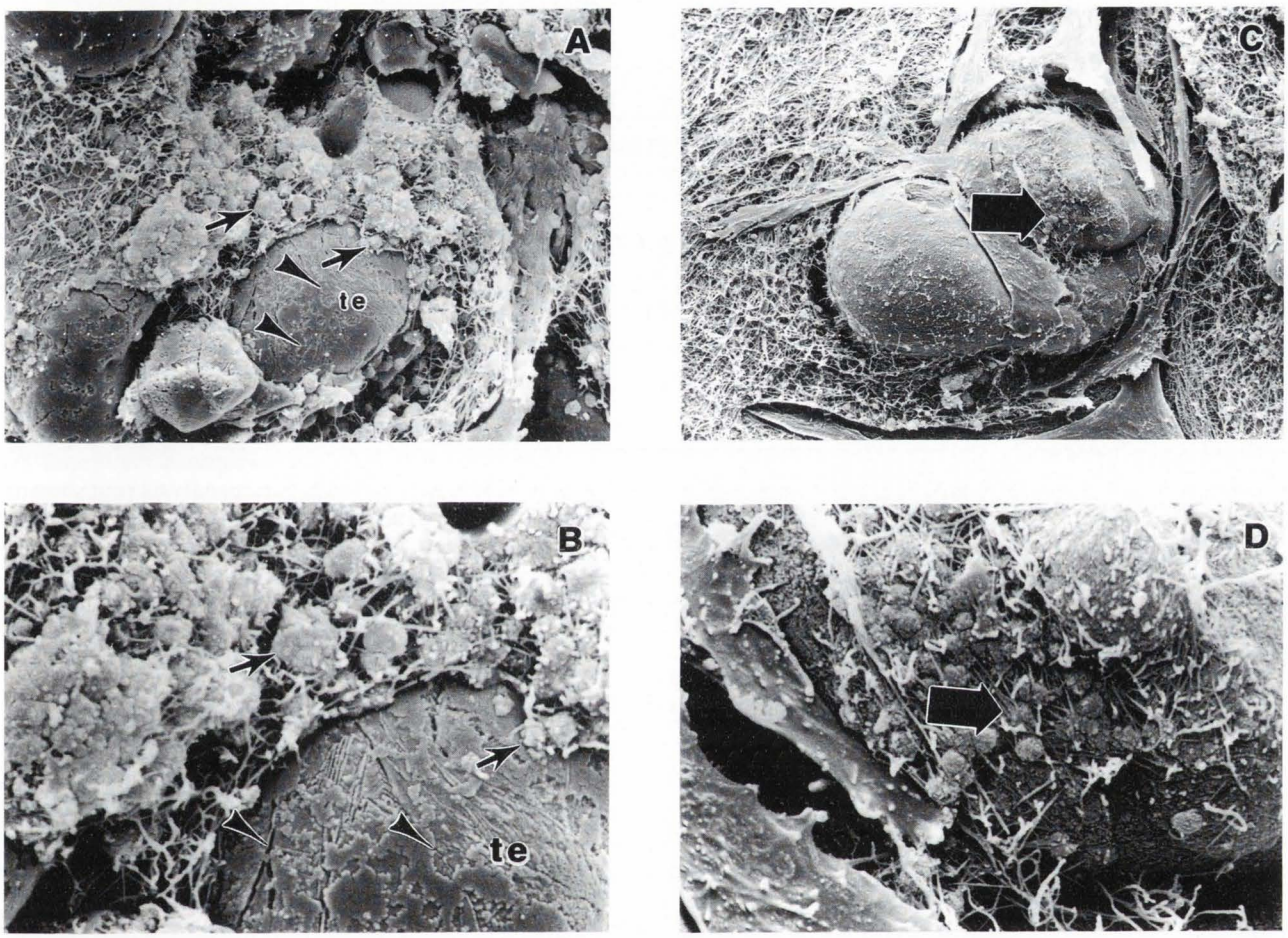

Figure 3. A and B. Scanning electron micrographs showing the deposition of globular material (arrows) on to the degrading tetracalcium phosphate (te) surface (arrowheads) after 2 weeks. **C and D.** Collagen fibres become incorporated with this interfacial layer at 4 weeks of culture (large arrows). Field widths: (A) 33.9 μm; (B) 13.4 μm; (C) 62.5 μm; and (D) 14.2 μm.

amorphous zone and the mineralized extracellular matrix. Specimens stained with ruthenium red revealed a higher staining intensity in the mineralized extracellular matrix as opposed to the amorphous zone (Figs. 4B and 4C). Collagen fibres, with their characteristic banding pattern, were seen both parallel and oblique to the amorphous zone which was, however, largely devoid of these fibres. Electron dense material, that sometimes contained calcium and phosphorous, was frequently seen in the amorphous zone (Fig. 4C).

Tricalcium phosphate

After 1 week of culture, SEM revealed widespread degradation of the tricalcium phosphate surface. Small cavities became apparent, which gave the plasma-sprayed surface a porous character. With TEM, a mineralized extracellular matrix was observed from 2 weeks onwards which was abundant at 4 weeks (Figs. 5A-5C). An amorphous layer was not seen at the mineralized tissue/tricalcium phosphate interface, while electron dense structures were only occasionally seen. Needle-shaped crystals from the mineralized extracellular matrix were intimately associated with the tricalcium phosphate. Degradation of the tricalcium phosphate surface resulted in crystallites that were surrounded by needle-shaped crystals (Fig. 5C). In other areas, needle-shaped crystals from the mineralized extracellular matrix were in direct contact with larger crystals of the tricalcium phosphate surface (Fig. 5B). They seemed to be strongly bound together, as ultrathin sectioning frequently resulted in a cutting artifact in the bulk tricalcium phosphate but not at the interface with the mineralized extracellular matrix (Fig. 5B). Ruthenium red staining revealed two structural arrangements at the tricalcium phosphate interface. One comprised collagen fibres interspersed with ruthenium red-positive material, in direct contact with its surface (Fig. 5D). The other consisted of ruthenium red-positive globular deposits that were directly formed onto the tricalcium phosphate surface and did not contain collagen fibres (Fig. 5D). Cellular processes were frequently associated with these deposits. After 8 weeks of

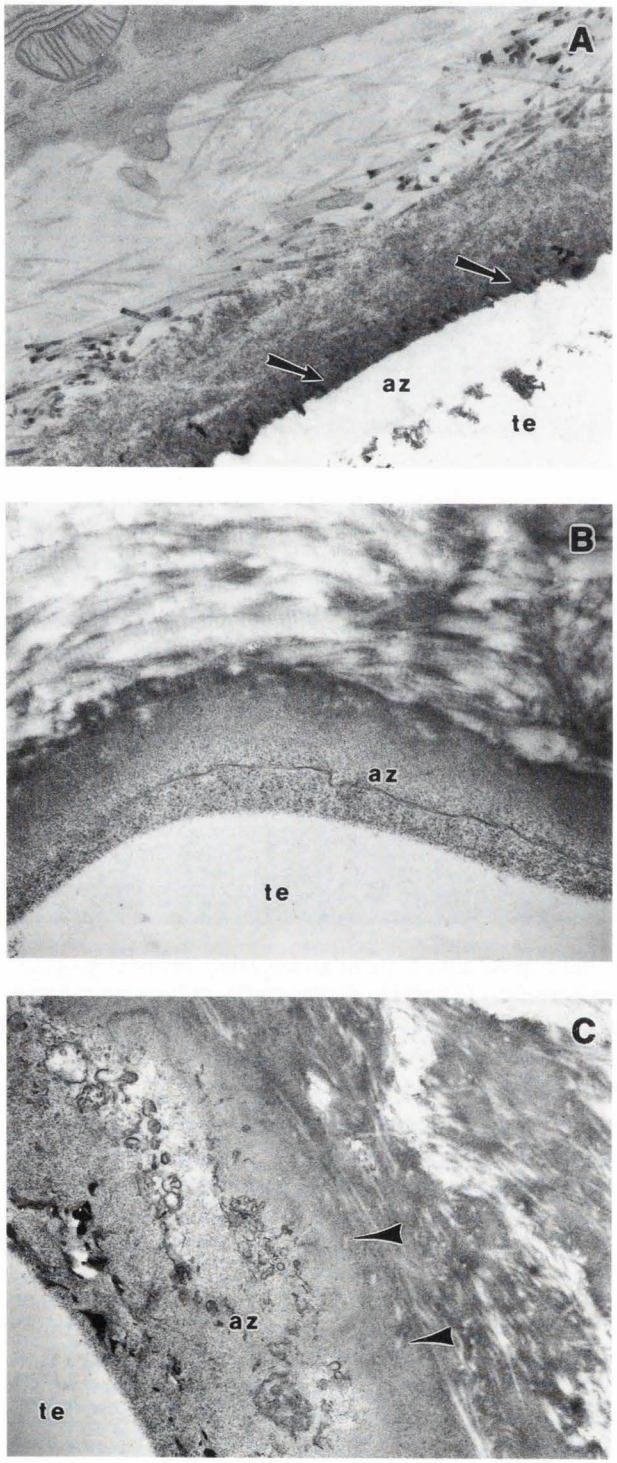

Figure 4. Transmission electron micrographs of tetracalcium phosphate (te), showing (**A**, 2 week culture) an undecalcified interface including an amorphous degradation zone (az) and an electron dense layer (arrows). **B and C** (4 week culture). Ruthenium red stained specimen revealing a faint staining in the collagen free amorphous zone, to which both parallel and obliquely aligned collagen fibres are attached (arrowheads). Field widths: (A) 6.6 μm; (B) 4.4 μm; and (C) 6.6 μm.

culture, some plasma-sprayed tricalcium phosphate particles were fully degraded, leaving only the crystallite boundaries visible (Fig. 6).

Magnesium whitlockite

Scanning electron microscopy revealed a severe degradation of the magnesium whitlockite surface already after 1 week of culture. This was confirmed with TEM that showed numerous highly degraded plasma-sprayed grains after 2 weeks of culture (Fig. 7A). The original surface of the plasma-sprayed particles was, however, still clearly visible. Mineralized extracellular matrix production could only be observed in limited areas. After 4 weeks of culture, numerous small particles were observed in the degrading magnesium whitlockite grains (Fig. 7B), that comprised aluminum and silicon, as revealed by X-ray microanalysis (not shown). After 8 weeks of culture, the formation of mineralized extracellular matrix was rarely observed on the magnesium whitlockite surface, which showed severe degradation as seen with SEM (Fig. 7C).

Discussion

The results of this study have shown three distinctly different interfacial structures that differed in the presence or absence of an electron dense layer and/or an amorphous zone. We have recently observed equivalent structures at the bony interface with various types of hydroxyapatite that differed in crystallinity, and concluded that the amorphous zone was the result of the rapid degradation of the hydroxyapatite surface [de Bruijn *et al.*, 1992b, 1993]. It is conceivable that the time in which a mineralized extracellular matrix is formed, is dependent on several factors. Firstly, the surface reactivity of a material must play a role in the mineralization process. This is confirmed by the results of this study in that fluorapatite, with its low solubility rate, shows the formation of a mineralized extracellular matrix on its surface after only 8 weeks of culture. Conversely, materials with higher solubility rates than fluorapatite, such as tricalcium phosphate, tetracalcium phosphate, and to a lesser extent, hydroxyapatite, already show the formation of a mineralized extracellular matrix after 2 weeks of culture. Although this is not in accordance with a report by Klein *et al.* (1991), who observed more connective tissue along the interface of tricalcium phosphate than around hydroxyapatite and tetracalcium phosphate when implanted in dog femora for 3 months, numerous other studies [Gatti *et al.*, 1990; Ikami *et al.*, 1990; Kotani *et al.*, 1991; Kitsugi *et al.*, 1993] have reported abundant new bone formation around tricalcium phosphate implants. Surface reactivity, however, is not only governed by the degradation rate of a material, but also by its ability to form a surface apatite layer. Since we have not studied this, we can only relate our observations to ultrastructural differences observed with the various materials. Another important factor which may be related to the occurrence of mineralization on a materials

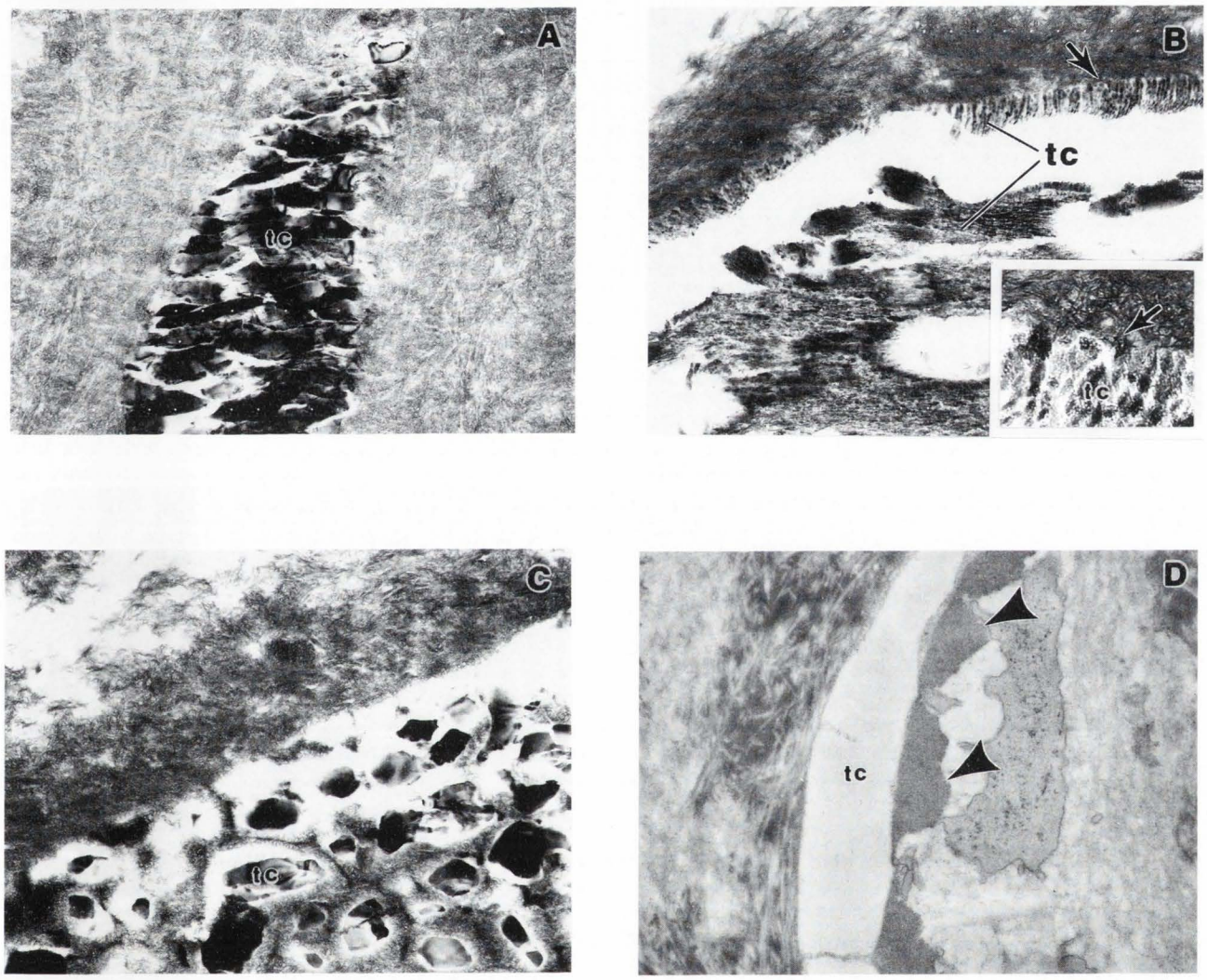

Figure 5. Transmission electron micrographs of undecalcified interfaces between tricalcium phosphate (tc) and the mineralized extracellular matrix. Needle shaped crystals from the matrix are intimately associated with tricalcium phosphate (tc) crystals (arrows and inset in **B**). **D**. Ruthenium red stained sample showing both afibrillar globular deposits (arrowheads), and mineralized extracellular matrix deposition to the tricalcium phosphate surface. Field widths: (A) 3.3 μm; (B) 5.7 μm; (C) 3.3 μm; and (D) 6.6 μm.

surface is the presence of trace elements such as aluminum and silicon. It has been reported that micromolar concentrations of aluminum ions could act directly on osteoblasts to stimulate their proliferation and differentiation [Lau *et al.*, 1991]. Aluminum ions might, therefore, stimulate bone formation *in vitro* [Lau *et al.*, 1991] and has been reported to induce *de novo* bone formation *in vivo* [Galceran *et al.*, 1987; Quarles *et al.*, 1990]. Higher concentrations of aluminum have, however, been reported to have adverse effects on mineralization processes, in that osteoid tissue remained unmineralized [Chan *et al.*, 1983]. Blumenthal and Posner (1984), and Blumenthal and Cosma (1992) have further shown that aluminum ions in solution *in vitro* slow the direct precipitation of hydroxyapatite, the transformation of amorphous calcium phosphate to hydroxyapatite, and the growth of hydroxyapatite seed crystals, all in a dose related manner. Thus, the substantial amount of aluminum in the magnesium whitlockite coating might have adversely affected the formation of a mineralized extracellular matrix on its surface. The absence of mineralization may also have been partially influenced by released magnesium ions which have similarly been reported to inhibit the formation and growth of hydroxyapatite crystals [Johnsson *et al.*, 1991; Blumenthal and Cosma, 1992]. However, a study by Ruggeri *et al.* (1987) did not show an adverse reaction with regard to mineralization processes around degrading particles of magnesium substituted ß-tricalcium phosphate. In contrast, they suggested that passive dissolution of this material

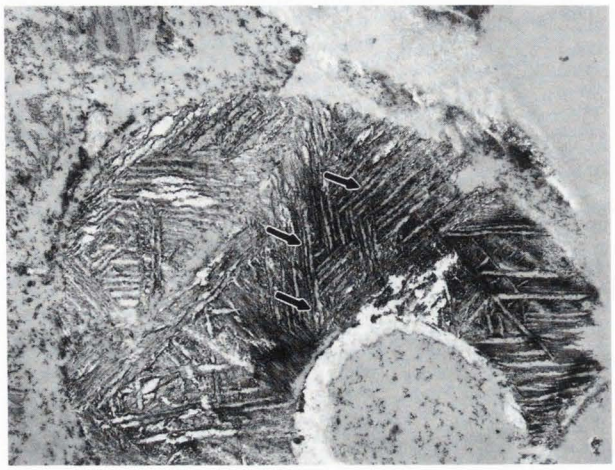

Figure 6. Transmission electron micrograph showing severe degradation of the tricalcium phosphate after 8 weeks of culture. Note the well defined crystallite boundaries (arrows). Field width: 9.4 μm.

accelerated the process of new bone formation. The presence of the trace elements, aluminum and silicon, may have been caused by the preparation method for powder production. Firstly, a large sintered block of magnesium whitlockite was produced and subsequently ground into particles, suitable for plasma-spraying; this was achieved using alumina beads which were mechanically stirred in a porcelain vessel. The aluminum could, therefore, have originated from the alumina beads, whereas the silicon may have been derived from the porcelain vessel. Although tricalcium phosphate was obtained from the same company and was prepared under identical conditions, it did not contain the above mentioned trace elements, which may be due to its lower degree of hardness and thus less wear of the alumina beads during the milling procedure. Since the other calcium phosphates were either reagent grade or spray dried, they did not contain large quantities of trace elements.

Interpretation of the various interfacial structures have been extensively discussed elsewhere, with regard to hydroxyapatite [de Bruijn *et al.*, 1992a], which may well be correlated to the materials studied herein. The electron dense layer is considered to represent protein adsorption, preceding or concurrently occurring with biological mineralization events on the initially stable surfaces of the plasma-sprayed calcium phosphates. The absence of the electron dense layer on tricalcium phosphate may be explained as a gradual degradation of the entire ceramic, resulting in an unstable surface for protein adsorption. In other words, proteins will have adsorbed on the tricalcium phosphate surface, however, as the latter progressed towards the centre of the bulk ceramic, no distinct deposition line would be seen. The amorphous zone is likely to represent two different mechanisms. The first was conclusively shown with various types of hydroxyapatite, examined in the same experimental system as described herein [de Bruijn *et al.*,

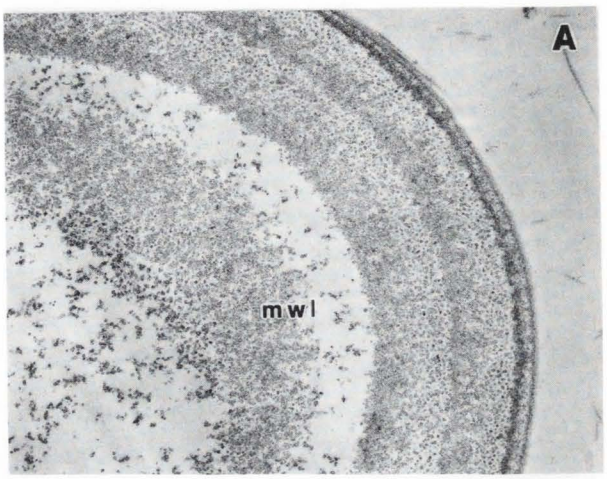

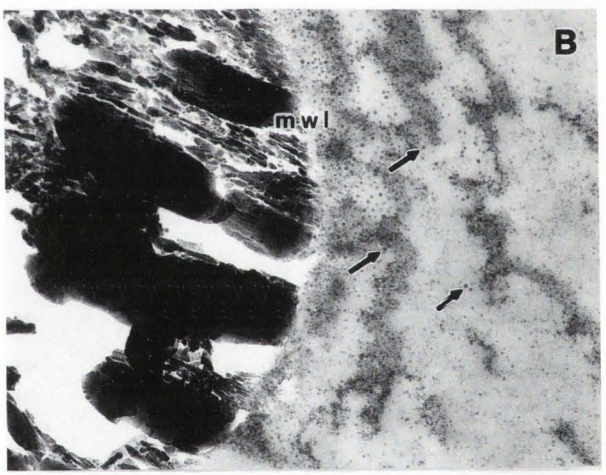

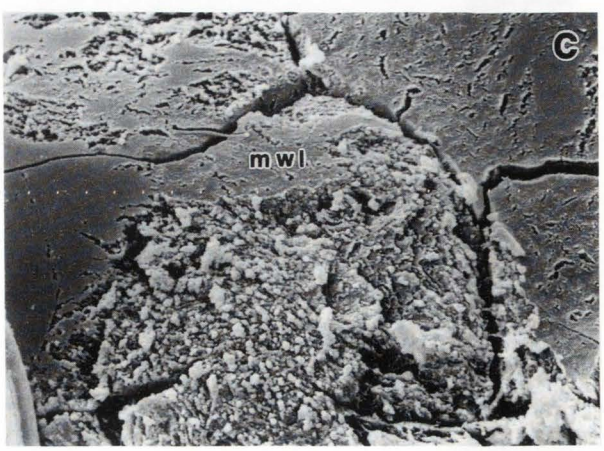

Figure 7. A and B. Transmission electron micrographs showing severe degradation of the magnesum whitlockite (mwl) coating. The small particles (arrows in **B**) were identified as aluminum and silicon containng, with X-ray microanalysis. **C**. The severe degradation and absence of mineralization on the magnesium whitlockie (mwl) surface could also be observed with SEM. Field vidths: (A) 6.6 μm; (B) 3.7 μm; and (C) 16.3 μm.

1992b, 1993], and represents degradation of the outer shell of the plasma-sprayed coating. During the plasma-spray process, the surface of the coating will cool down relatively quickly, as compared to the underlying bulk of the coating, resulting in the formation of an amorphous phase. This is, however, only true for calcium phosphates with a low thermal stability. Fluorapatite for example, has a superior thermal stability than hydroxyapatite [Lugscheider *et al.*, 1988] and will, therefore, not form an amorphous phase at its surface. Despite the fact that the plasma-sprayed hydroxyapatite revealed a pure "apatitic" phase with X-ray diffraction, recent studies of Paschalis and Nancollas (1992) have indicated that they are likely to contain other calcium phosphate phases as well, which may have profound effects on their surface reactivity, and thus, on their interfacial arrangement with bone tissue. A similar multi-phasic character may have occurred on the other plasma-sprayed materials such as tetracalcium phosphate [Klein *et al.*, 1991]. The second mechanism comprises biological events, in that afibrillar mineralization globules are formed at early stages of bone formation [Davies *et al.*, 1991; de Bruijn *et al.*, 1992a]. These globular accretions are clearly seen in Figure 5D and contain glycosaminoglycan positive material. Subsequent fusion with the degrading ceramic surface will, therefore, result in an interface as shown in Figures 1B, 4B and 4C, in which a gradual transition of ruthenium red positive material is shown from the mineralized extracellular matrix to the hydroxyapatite surface.

Concluding, it can be said that bone-calcium phosphate interface reactions are not only influenced by the crystallinity [de Bruijn *et al.*, 1992b, 1993], but also by the chemical composition of calcium phosphates. Furthermore, it is feasible that the degradation rate of calcium phosphate ceramics is important for the rate in which the interface is formed.

Acknowledgements

The authors thank Mr. G. Beckers {National Ceramic Centre (ECN), Petten, The Netherlands} for supplying tricalcium phosphate and magnesium whitlockite, Joop Wolke (Biomaterials Department) and Jan Flach (CAM-Implants B.V., Leiden) for plasma spraying the various materials, and they acknowledge Lambert Verschragen for printing the photographic material and Yvonne Bovell for english text corrections.

References

Blumenthal NC, Posner AC (1984) In vitro model of aluminum-induced osteomalacia: inhibition of hydroxyapatite formation and growth. Calc. Tiss. Int. **36**, 439-447.

Blumenthal NC, Cosma MS (1992) Effects of metal ions on apatite formation and bone mineralization. In: Tissue-Inducing Biomaterials. Cima L, Ron E (eds.). Mat. Res. Soc. Symp. Proc. **252**. Materials Res. Soc., Pittsburgh, PA. pp. 29-35.

Chan YL, Alfrey AC, Posner S, Lissner D, Hille E, Dunstan CR, Evans RA (1983) Effect of aluminum on normal and uremic rats: tissue distribution, vitamin D metabolites, and quantitative bone histology. Calc. Tiss. Int. **35**, 344-352.

Davies JE, Chernecky R, Lowenberg B, Shiga A (1991) Deposition and resorption of calcified matrix *in vitro* by rat bone marrow cells. Cells and Materials **1**, 3-15.

de Bruijn JD, Klein CPAT, de Groot K, van Blitterswijk CA (1992a) The ultrastructure of the bone-hydroxyapatite interface in vitro. J. Biomed. Mater. Res. **26**, 1365-1382.

de Bruijn JD, Davies JE, Flach JS, de Groot K, van Blitterswijk CA (1992b) Ultrastructure of the mineralized tissue/calcium phosphate interface in vitro. In: Tissue-Inducing Biomaterials. Cima L, Ron E (eds). Mat. Res. Soc. Symp. Proc. **252**. Materials Res. Soc., Pittsburgh, PA. pp. 63-70.

de Bruijn JD, Flach JS, de Groot K, van Blitterswijk CA, Davies JE (1993) Analysis of the bony interface with various types of hydroxyapatite *in vitro*. Cells and Materials **3(2)**, 115-127.

de Groot K, Klein CPAT, Driessen AA (1985) Calcium phosphate bioceramics. J. Head & Neck Pathol. **4**, 90-93.

Dhert WJA, Klein CPAT, Jansen JA, van der Velde EA, Vriesde RC, Rozing PM, de Groot K (1993) A histological and histomorphometrical investigation of fluorapatite, magnesium whitlockite and hydroxylapatite plasma-sprayed coatings in goats. J. Biomed. Mater. Res. **27**, 127-138.

Driessens FCM (1988) Physiology of hard tissues in comparison with the solubility of synthetic calcium phosphates. Ann. N.Y. Acad. Sci. **523**, 131-136.

Galceran T, Finch J, Bergfeld M, Coburn J, Martin K, Teitelbaum S, Slatopolski E (1987) Biological effects of aluminum on normal dogs: studies on the isolated perfused bone. Endocrinol. **121**, 406-413.

Ganeles J, Listgarten MA, Evian CI (1985) Ultrastructure of durapatite-periodontal tissue interface in human intrabony defects. J. Periodontol. **57**, 133-139.

Gatti AM, Zaffe D, Poli GP (1990) Behaviour of tricalcium phosphate and hydroxyapatite granules in sheep bone defects. Biomaterials **11**, 513-517.

Heling I, Heindel R, Merin B (1981) Calcium-fluorapatite. A new material for bone implants. J. Oral Implantol. **9**, 548-555.

Ikami K, Iwaku M, Ozawa H (1990) An ultrastructural study of the process of hard tissue formation in amputated dental pulp dressed with α-tricalcium phosphate. Arch. Histol. Cytol. **53**, 227-243.

Jarcho M (1981) Calcium phosphate ceramics as hard tissue prosthetics. Clin. Orthop. Relat. Res. **157**, 259-278.

Johnsson MSA, Paschalis E, Nancollas GH (1991) Kinetics of mineralization, demineralization, and transformation of calcium phosphates at mineral and protein surfaces. In: The Bone-Biomaterial Interface. Davies JE

(ed.). University of Toronto Press, Toronto, Canada. pp. 68-75.

Kitsugi T, Yamamuro T, Nakamura T, Kotani S, Kokubo T, Takeuchi H (1993) Four calcium phosphate ceramics as bone substitutes for non-weight bearing. Biomaterials **14**, 216-224.

Klein CPAT, Driessen AA, de Groot K (1983) Biodegradation behaviour of various calcium phosphate materials in bone tissue. J. Biomed. Mater. Res. **17**, 769-778.

Klein CPAT, de Groot K, Driessen AA, van der Lubbe HBM (1986) A comparative study of different ß-whitlockite ceramics in rat cortical bone with regard to their biodegradation behaviour. Biomaterials **7**, 144-146.

Klein CPAT, Patka P, van der Lubbe HBM, Wolke JGC, de Groot K (1991) Plasma-sprayed coatings of tetracalcium phosphate, hydroxyl-apatite, and α-TCP on titanium alloy: An interface study. J. Biomed. Mater. Res. **25**, 53-65.

Kotani S, Fujita Y, Kitsugi T, Nakamura T, Yamamuro T (1991) Bone bonding mechanism of ß-tricalcium phosphate. J. Biomed. Mater. Res. **25**, 1303-1315.

Lau KH, Yoo A, Ping Wang S (1991) Aluminum stimulates the proliferation and differentiation of osteoblasts *in vitro* that is different from fluoride. Mol. Cell. Biochem. **105**, 93-105.

LeGeros RZ (1981) Apatites in biological systems. Prog. Crystal Growth Char. **4**, 1-45.

LeGeros RZ (1988) Calcium phosphate materials in restorative dentistry: A review. Adv. Dent. Res. **2**, 164-180.

Luft JH (1971) Ruthenium red and violet. II. Animal tissues. Anat. Rec. **171**, 369-415.

Lugscheider E, Weber Th, Knepper M (1988) Production of biocompatible coatings of hydroxyapatite and fluorapatite. In: Proc. National Thermal Spray Conference. Am. Soc. Metals, Metals Park, OH. p. 87 (abstract).

Maniatopoulos C, Sodek J, Melcher AH (1988) Bone formation *in vitro* by stromal cells obtained from bone marrow of young adult rats. Cell Tissue Res. **254**, 317-330.

Moreno EC, Kresak M, Zahradnik RT (1977) Physicochemical aspects of fluoride apatite systems relevant to the study of dental caries. Caries Res. **11 (suppl. 1)**, 142-146.

Paschalis EP, Nancollas GH (1992) Dual constant composition kinetics studies of the demineralization of ceramic plasma coated apatite surfaces. In: Tissue-Inducing Biomaterials. Cima L, Ron E (eds). Mat. Res. Soc. Symp. Proc. **252**. Materials Res. Soc., Pittsburgh, PA. pp. 17-21.

Quarles LD, Murphy G, Vogler JB, Drezner MK (1990) Aluminum-induced neo-osteogenesis: a generalized process affecting trabecular network in the axial skeleton. J. Bone Miner. Res. **5**, 625-635.

Ruggeri A, Franchi M, Evangelisti A, de Pasquale V, Bigi A, Ripamonti A, Roveri N (1987) Morphological studies of new bone formation favoured by ß-TCP implants. In: Biomaterials in Clinical Applications. Pizzoferrato A, Marchetti PG, Ravaglioli A, Lee AJC (eds.). Elsevier, Amsterdam. pp. 603-608.

van Blitterswijk CA, Grote JJ, Kuijpers W, Blok-van Hoek CJG, Daems WTh (1985) Bioreactions at the tissue/hydroxyapatite interface. Biomaterials **6**, 243-251.

Discussion with Reviewers

R.Z. LeGeros: It is known that the coating obtained when plasma-spraying hydroxyapatite (HA) consists principally of HA, amorphous calcium phosphate (ACP) in varying ACP/HA ratios, and smaller amounts of other phases {e.g. α- and ß-tricalcium phosphate (TCP), tetracalcium phosphate (TECP), calcium oxide}. The composition and crystallinity of the coating influences its biodegradation. Do you have information on the coating composition (e.g., ACP/HA ratio, other calcium phosphate phases or calcium oxide present) and crystallinity (of the HA phase) for each of the plasma-sprayed materials (HA, FA, TECP, and Mg-substituted whitlockite)?
Authors: The information you request for each of the coatings is as follows: **Hydroxyapatite**: approximately 60% crystalline HA and no other detectable phases except ACP. **Fluorapatite**: approximately 90% crystalline and no other detectable phases except ACP. **Tricalcium phosphate**: approximately 90% crystalline in the form of α-TCP. **Tetracalcium phosphate**: approximately 90% crystalline and no other detectable phases except ACP. **Magnesium whitlockite**: approximately 60% crystalline in the form of α-TCP, other phase is ACP. A detailed method regarding crystallinity determination has been recently published in this journal (de Bruijn *et al.*, 1993).

A.M. Gatti: Are you sure that the differences in behaviour are due only to the chemical composition/crystal structure of the materials? Did you measure the final surface roughnesses of the samples in order to exclude this factor?
P. Thomsen: What are the surface roughnesses of the plasma-sprayed surfaces? If so, could the authors briefly comment if part of the observations might be related to such differences in surface microtopography?
J.L. Ricci: Nodule formation, leading to mineralization, is based on the formation of high density cultures, and surface texture can play a role in controlling the growth rates of attached cells. Thus, it may be possible to influence rates of mineral formation through differences in cell growth rates on surfaces of different roughnesses. Did you observe noticeable differences in cell growth and could you comment on differences in surface texture?
Authors: The surface roughness (Ra) of the examined plasma-sprayed calcium phosphates was approximately 4 μm. The observed differences in extracellular matrix formation are, therefore, only due to variation in

chemical composition and crystal structure of the materials. Although no noticeable differences in cell growth were seen, there were differences in cellular attachment on MWL and tissue culture polystyrene, especially after long culture times (see next answer also).

N.C. Blumenthal: The principal concern of this reviewer is the lack of characterization of the surface by X-ray diffraction and/or infrared spectroscopy. The authors assume that the surfaces are exactly what the suppliers state they are. This point is crucial since the central theme of the paper is the influence of surfaces, both chemically and crystallographically on the formation of a mineralized interface. Some structural and/or chemical characterization of the surface appears to be necessary to draw conclusions from the **Results**.
Authors: Kindly see our two answers above.

P. Thomsen: The authors report that cells were lost on magnesium whitlockite and tissue culture polystyrene. Do the authors have any further data and a possible explanation for this observation? Are there material-related differences in cell adhesion and spreading to the various substrata after 1 and 2 weeks?
Authors: The only differences seen in cell adhesion on the various materials was at longer culture times. A similar phenomenon has been observed on tissue culture polystyrene and related to the amount of inoculated cells and the absence of extracellular matrix bonding to the substratum (Y.P. Bovell, personal communication). The differences we observed may be due to the formation and attachment of the extracellular matrix to the various substrata. Since this was absent on magnesium whitlockite and tissue culture polystyrene, this might explain the weak cellular adhesion to these substrata.

P. Thomsen: What is the particle size distribution and degree of crystallinity for the various calcium phosphates?
Authors: Both the hydroxyapatite and fluorapatite were spray-dried powders with a particle sizes ranging from 20 to 40 μm. The tricalcium phosphate and magnesium whitlockite were irregular ground powders with particle sizes of 25 to 50 μm and 45 to 71 μm, respectively. The tetracalcium phosphate had a particle size of < 125 μm. Please also see the answer to the first question of Dr. LeGeros, regarding the crystallinities of the various calcium phosphate coatings.

P. Thomsen: The average width of the amorphous zone at TECP is 800 nm. In Figure 4C, the zone appears to be about 4-fold larger in width than the average zone. Do the authors have any further observations with regard to variations of the zone (for instance, the width and contents) in relation to material and/or time? How do the ultrastructural characteristics and dimensions of the amorphous zones at HA and TECP relate to previous *in vitro* and *in vivo* observations on non-collagenous amorphous zones at biomaterial surfaces?

Authors: Since there was a large variability in size of the interfacial structures, there is no clear relation between the width of the amorphous zone, the material used (HA or TECP), and the time. This variability is due to the degrading character of the substratum. The width of the non-collagenous zones at various biomaterial surfaces *in vitro* and *in vivo* varies from a few nanometers to 1 μm (de Bruijn *et al.*, 1993).

J.L. Ricci: Davies *et al.* (1991) and your group [de Bruijn *et al.* (1992a)] have shown evidence that mineral production in this model is cell-mediated. Yet, in a closed system such as this, even with change of cell culture medium every other day, it would be possible for dissolution of the experimental surface to raise calcium and phosphate levels to the point where direct precipitation of mineral would occur using the surface as a substrate. Figure 2B suggests this type of surface reaction. This type of dissolution followed by reprecipitation has been shown for a number of different types of bioactive surfaces incubated in simulated body fluids. Have you monitored calcium and phosphate levels in the medium, or perhaps incubated these substrates in the cell culture medium, in the absence of cells, and examined the surfaces for the type of ultrastructure you have described? Could you comment on how much of the observed mineralization is cell-mediated and how much is physical/chemical precipitation?
Authors: Our controls were the different substrata that were soaked in culture medium without the presence of cells. In these controls, we have never observed precipitation. The observed mineralization is thus solely due to the presence of cells.

U.M. Gross: What is the leading mechanism for bone bonding: the deposition of mineral globules as shown by Davies *et al.* (1991) or the degradation and reprecipitation of some mineral as mentioned in your present paper?
Authors: The capacity of bone to bond with biomaterials is based on the ability of the latter to generate a surface apatite layer. This surface apatite layer is formed by degradation, (re)precipitation, and/or epitaxial crystal growth. Subsequent co-precipitation and/or incorporation of proteins such as glycosaminoglycans, osteocalcin and osteopontin, and the deposition of afibrillar mineralized globular accretions, will give rise to bone bonding.